

# STOCHASTIC ADAPTIVE TRACKER BASED ON NOISE-CORRUPTED SPACE-TIME MEASUREMENT PROCESS

Bruce A. Johnson and Peter S. Maybeck

Department of Electrical and Computer Engineering  
Air Force Institute of Technology  
Wright-Patterson AFB, OH 45433

## ABSTRACT

A multiple model adaptive estimator (MMAE) is formulated to estimate the state of a dynamic system modeled by a linear stochastic differential equation, from which the feedback observations are described as a noise-corrupted Poisson space-time point process. Then the MMAE is embedded into a stochastic adaptive PI tracker using LQG and assumed certainty equivalence techniques, and the MMAE, the Kalman filter (used to estimate the target state) and the tracker are evaluated for parameter sensitivity, robustness, and adaptation using Monte Carlo simulation.

## INTRODUCTION

The proposed problem is an adaptive tracker system that is adequately modeled by a linear stochastic differential equation from which the feedback observations are modeled as a noise-corrupted space-time point process and where the time to the next observation is Poisson distributed and unknown a priori. One application of such a model structure is for the estimation and control of a neutral particle beam.

A method for sensing the beam's centroid has been proposed in which the beam is illuminated by one or more lasers [11]. At certain angles of intersection and at different particle velocities, the particle electrons absorb photons from the laser beam and attain a higher energy state. When the particle beam electrons relax and spontaneously decay to their ground energy state, they expend the energy as light. By detecting the light energy, the position of the beam can be inferred. If the light energy were to arrive at the photo-detector at a sufficient signal rate as to produce an observable current, it might be modeled by a continuous-time, Gaussian process as done in many communication and control type problems. But, the assumption upon which this research is based is that the photon events do not arrive at such a sufficient rate. Instead, a discrete, Poisson space-time process is used to describe the arrival of the individual signal-induced events (the photons) and the noise-induced events (caused by dark currents within the detector, or other outside sources of noise). The time between events will be described by a conditional Poisson process (conditioned on the arrival rate parameter), and the model for event location on the

detector plane is composed of Gaussian spatially distributed signal-induced events, and uniformly distributed noise-induced events.

An overview of the tracker design that is used throughout this research is shown in Fig. 1. The purpose of a tracker is to generate a control input,  $u(t_i)$ , that minimizes the tracking error,  $e(t)$ , which is defined as the difference between the the controlled variable,  $y_c(t)$ , and the reference (i.e., target) variable,  $y_r(t)$ .

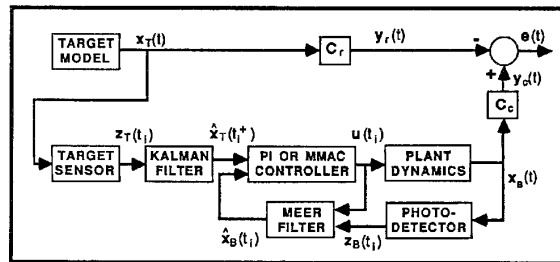


Figure 1. System Overview

The target model is generated through a shaping filter which produces an exponentially time-correlated noise process to simulate the target acceleration. The target sensor is modeled as a sample and hold device that obtains a noise-corrupted measurement of the target's position,  $z_T(t_i)$ , at a regular, prespecified sample rate. The measurements are used by the Kalman filter to generate a target state estimate,  $\hat{x}_T$ .

The particle beam dynamics are modeled as an exponentially time-correlated position process, the output of a shaping filter having one dominant pole. The position of the beam is inferred through the observations detected at the surface of the photo-detector. These observations,  $z_B(t)$ , are assumed to be well modeled by a Poisson space-time point process, and can be of either signal or noise origin.

The Meer filter [8,9] is an optimal Bayesian filter designed to discriminate between the signal- and noise-induced events, and generate a beam state estimate,  $\hat{x}_B(t_i)$ , from the signal-induced events. This is accomplished through a multiple model structure

composed of a bank of Snyder-Fishman filters (see Fig. 2) [1,5]. The Snyder-Fishman filter is a minimum-mean square estimator that estimates the position of maximum intensity from the arrival of the signal-induced events. In the absence of noise-induced events, the Snyder-Fishman filter provides good results; however, the performance of such estimators and/or controllers is seriously degraded by unmodeled appearance of noise-induced observations [10]. Although it is possible to improve this performance through the use of residual monitoring techniques, such as are commonly exploited in practical Kalman filters [5,10], it is desirable to establish an adaptive estimator such as the Meer filter with enhanced performance potential. The different hypothesis sequences used in the Meer filter define the different possible sequences of signal- and noise-induced events, and each elemental filter is allowed to process the observed events only when its associated hypothesis has defined the event as being signal-induced.

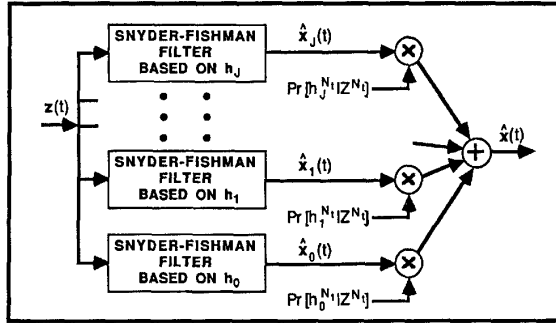


Figure 2. Multiple Model Adaptive Estimator

The target state estimate and the beam state estimate are fed into the discrete-time controller algorithm to generate a command input to the plant. Because the target and the beam processes are assumed to be well modeled as Gaussian processes as produced by linear shaping filters, "nearly" optimal controller designs can be developed using the linear quadratic (LQ) full-state feedback controller synthesis process, and the assumed certainty equivalence technique [6] for incorporating filters into the loop. A proportional-plus-integral (PI) controller (selected because of its ability to handle unmodeled constant disturbances that arise from linearized models) was developed and evaluated on its own merit and within an adaptive multiple model controller structure.

#### ESTIMATING THE BEAM POSITION

The position of the beam is inferred from the spatial detection of the individual photoelectron events caused by the resonant scattering of light energy. The signal-induced events can be modeled as a Poisson space-time point process on  $[t_0, \infty) \times R^M$ . Each event has associated with it the time of occurrence  $t \in [t_0, \infty)$ , and a

spatial location  $r \in R^M$ . The rate of occurrence is defined as the signal rate parameter,  $\lambda_S(t, r, x(t))$ , and is assumed to have a spatial Gaussian function given as:

$$\lambda_S(t, r, x(t)) = \Lambda(t) \exp\{-[r - H(t)x(t)]^T R^{-1}(t)[r - H(t)x(t)]/2\} \quad (1)$$

where

$\Lambda(t)$  is the maximum amplitude of the rate function  
 $R$  is a symmetric positive definite matrix defining the spread of the beam  
 $r$  is a spatial location on the detector array  
 $H(t)x(t)$  is the signal-induced beam centroid in  $R^M$   
 $x(t)$  is a stochastic process defining the state dynamics of the beam centroid  
 $H(t)$  is an  $m \times n$  projection matrix from the state space into the space of measured photoelectron events

The beam's spatial Gaussian function is a result of the diffusion and spreading of the beam. The noise-induced events are modeled as a Poisson space-time point process on  $[t_0, \infty) \times R^M$  with a noise rate parameter,  $\lambda_N(t, r)$ . The noise process is assumed to be statistically independent of the signal process [9]. The noise events are assumed to be uniformly distributed over the detector's field of view. The ratio between the average rate of arrival of signal- and noise-induced events is the signal-to-noise ratio. Because both the signal and noise processes are Poisson point processes and independent of one another, their sum remains a Poisson point process, with rate parameter:

$$\lambda(t, r(t), x(t)) = \lambda_S(t, r(t), x(t)) + \lambda_N(t, r(t)) \quad (2)$$

Snyder and Fishman developed an estimator which specifically handles the case of measurements that appear as a Poisson point process [12], and the state dynamics assumed to satisfy,

$$dx(t) = F(t)x(t)dt + B(t)u(t)dt + G(t)d\beta(t) \quad (3)$$

where  $\beta$  is Brownian motion of diffusion  $Q(t)=I$ . In the absence of noise-induced events, the Snyder-Fishman filter estimates the beam's centroid as  $H(t)\hat{x}(t)$ , where  $\hat{x}(t)$  is the expected value of the beam states,  $x(t)$ , conditioned on all the previous measurements. The filter is described by the following stochastic differential equations [8,12]:

$$d\hat{x}(t) = F(t)\hat{x}(t)dt + B(t)u(t)dt + \int_{R^M} K(t)[r - H(t)\hat{x}(t)] \cdot N(dt \times dr) \quad (4)$$

$$dP(t) = F(t)P(t)dt + P(t)F^T(t)dt + G(t)G^T(t)dt - \int_{R^M} K(t)H(t)P(t)N(dt \times dr) \quad (5)$$

$$K(t) = P(t)H^T(t)[H(t)P(t)H^T(t) + R(t)]^{-1} \quad (6)$$

where

$\hat{\mathbf{x}}(t_0) = \mathbf{x}_0$  and  $\mathbf{P}(t_0) = \mathbf{P}_0$  are the initial conditions  
 $\mathbf{P}(t)$  is the filter-computed error covariance  
 $\mathbf{G}(t)\mathbf{G}^T(t) = \mathbf{G}(t)\mathbf{Q}(t)\mathbf{G}^T(t)$ ;  $\mathbf{Q}(t) = \mathbf{I}$   
 $\mathbf{K}(t)$  is the filter gain

The notation found in Eqs. (4) and (5) involves counting integrals, where

$$\int_{R^M} f(t, \mathbf{r}) N(d\mathbf{t} \times d\mathbf{r}) = \begin{cases} 0 & N_t = 0 \\ \sum_{i=1}^{N_t} f(t_i, \mathbf{r}_i) \delta(t, t_i) & N_t \geq 1 \end{cases}$$

and  $\delta(t, t_i)$  is a Kronecker delta. If no events are detected, then the integral equals zero. If an event is detected, the integral causes a jump discontinuity,  $f(t, \mathbf{r})$ , to be added to the solution of the differential equation for time  $t_i$  [12].

The propagation and update equations can be derived from Eqs. (4) and (5). The propagating equations to be used between (signal-induced) events are:

$$d\hat{\mathbf{x}}(t) = \mathbf{F}(t)\hat{\mathbf{x}}(t)dt + \mathbf{B}(t)\mathbf{u}(t)dt \quad (7)$$

$$d\mathbf{P}(t) = \mathbf{F}(t)\mathbf{P}(t)dt + \mathbf{P}(t)\mathbf{F}^T(t)dt + \mathbf{G}(t)\mathbf{G}^T(t)dt \quad (8)$$

When an event has been detected, a measurement update can take place as defined by the following equations:

$$\hat{\mathbf{x}}(t_i^+) = \hat{\mathbf{x}}(t_i^-) + \mathbf{K}(t_i)[\mathbf{r}_i - \mathbf{H}(t_i)\hat{\mathbf{x}}(t_i^-)] \quad (9)$$

$$\mathbf{P}(t_i^+) = \mathbf{P}(t_i^-) - \mathbf{K}(t_i)\mathbf{H}(t_i)\mathbf{P}(t_i^-) \quad (10)$$

where the Snyder-Fishman filter gain is defined by

$$\mathbf{K}(t_i) = \mathbf{P}(t_i^-)\mathbf{H}^T(t_i)[\mathbf{H}(t_i)\mathbf{P}(t_i^-)\mathbf{H}^T(t_i) + \mathbf{R}(t_i)]^{-1} \quad (11)$$

Equations (7) through (11) appear strikingly similar to the Kalman filter equations, except the measurement update times are not known a priori [12]. Instead, the measurement updates occur whenever an event is detected, and the time interval is defined as a Poisson process.

To incorporate the noise-induced events, a Bayesian filter was developed by Meer [8,9]. It is composed of a bank of Snyder-Fishman filters, where each elemental filter is assigned to a hypothesis sequence. Each hypothesis within the sequence defines which events are assumed to be signal-induced and which were noise-induced. The elemental Snyder-Fishman filters are updated on arrival of the hypothesized signal-induced events.

The state estimate out of each filter is defined as,

$$\hat{\mathbf{x}}_j(t) = E\{\mathbf{x}(t)|h_j^{N_t}Z^{N_t}\} \quad (12)$$

where  $\hat{\mathbf{x}}_j(t)$  is the expected value of the beam states,  $\mathbf{x}_j(t)$ , conditioned on the  $j$ -th assumed hypothesis time history,  $h_j^{N_t}$ , and the observations history,  $Z^{N_t}$ , of events  $(t_i, \mathbf{r}_i)$ , where  $i = 1, 2, \dots, N_t$ . Then, each sequence is probabilistically weighted and the weighted sum of all the elemental filter states is used to estimate the location of the beam centroid,

$$\hat{\mathbf{x}}(t) = \sum_{j=1}^{2^{N_t-1}} \text{Pr}[h_j^{N_t}|Z^{N_t}] \cdot \hat{\mathbf{x}}_j(t) \quad (13)$$

with a Meer filter computed error covariance defined as

$$\mathbf{P}(t) = \sum_{j=1}^{2^{N_t-1}} \text{Pr}[h_j^{N_t}|Z^{N_t}] \cdot \{\mathbf{P}_j(t) + [\hat{\mathbf{x}}_j(t) - \hat{\mathbf{x}}(t)][\hat{\mathbf{x}}_j(t) - \hat{\mathbf{x}}(t)]^T\} \quad (14)$$

The weighting probabilities,  $\text{Pr}[h_j^{N_t}|Z^{N_t}]$ , are the conditional probabilities that a hypothesis sequence is correct, conditioned of the measurement history that has been observed.

The weighting probability starts at  $t_0$ , with  $\text{Pr}[h_j^0|Z^0] = 1$ . The subsequent weighting probabilities appear as:

$$\text{Pr}[h_j^{N_t}|Z^{N_t}] = \frac{\lambda_S(t_k, \mathbf{r}_k, \hat{\mathbf{x}}(t_k)) \text{ or } \lambda_N(t_k, \mathbf{r}_k)}{\lambda(t_k, \mathbf{r}_k, \hat{\mathbf{x}}(t_k))} \cdot \text{Pr}[h_j^{N_t-1}|Z^{N_t-1}] \quad (15)$$

where  $\lambda_S(t_k, \mathbf{r}_k, \hat{\mathbf{x}}(t_k))$ ,  $\lambda_N(t_k, \mathbf{r}_k)$  and  $\lambda(t_k, \mathbf{r}_k, \hat{\mathbf{x}}(t_k))$  are estimates of the signal, noise and total rate parameters. The estimate of the signal rate parameter appears in the numerator for an assumed signal-induced event, and is found by evaluating Eq. (1) for  $\mathbf{x}(t) = \hat{\mathbf{x}}(t)$ . The estimate of the noise rate parameter is used for an assumed noise-induced event. Because of the recursive nature of Eq. (15), only knowledge of the most recent measurement is needed, rather than a growing memory of the entire history of measurements, for its evaluation [9].

With the arrival of each new measurement, the number of hypothesis sequences double to account for the possibility that the event could be of either signal or noise origin. To prevent the filter from growing to an unmanageable size, the filter depth,  $D$ , is limited by a pruning algorithm referred to as the "merge" method [8]. The hypothesis sequences that are identical to each other in the assumptions made over the  $D-1$  most recent events are paired up. That is, the members of each pair of hypothesis sequences differ by the assumption made about the oldest event in the current sequence, and when the sequences are merged, the oldest event is dropped. The state estimates and error covariances

associated with each merged pair can be found using the following equations:

$$\hat{\mathbf{x}}_j'(t) = \{Pr[h_j|Z^{N_j}] \cdot \hat{\mathbf{x}}_j(t) + Pr[h_k|Z^{N_k}] \cdot \hat{\mathbf{x}}_k(t)\} / A \quad (16)$$

$$\mathbf{P}_j'(t) = \{Pr[h_j|Z^{N_j}] \cdot (\mathbf{P}_j(t) + [\hat{\mathbf{x}}_j(t) - \hat{\mathbf{x}}_j'(t)][\hat{\mathbf{x}}_j(t) - \hat{\mathbf{x}}_j'(t)]^T) + Pr[h_k|Z^{N_k}] \cdot (\mathbf{P}_k(t) + [\hat{\mathbf{x}}_k(t) - \hat{\mathbf{x}}_j'(t)][\hat{\mathbf{x}}_k(t) - \hat{\mathbf{x}}_j'(t)]^T)\} / A \quad (17)$$

$$A = Pr[h_j|Z^{N_j}] = Pr[h_j|Z^{N_j}] + Pr[h_k|Z^{N_k}] \quad (18)$$

where

$h_j^D$  and  $h_k^D$  denote the two different sequences being merged into the new single sequence  $h_j^D$ :  $k = j + 2^D$  and  $j = 0, 1, \dots, (2^D - 1)$   
 $D$  is the memory depth after pruning has occurred  
 $\hat{\mathbf{x}}_j'$  and  $\mathbf{P}_j'$  are the "merged" state estimates and error covariances as the number of elemental filters are reduced from  $2^{D+1}$  to  $2^D$

The division by  $A$  in Eq. (16) yields normalization so that the sum of the probabilities of each new estimate equals one.

A performance analysis on the Meer filter found the Meer filter virtually insensitive to the depth parameter  $D$ . Varying  $D$  from  $D=1$  to  $D=8$  produced less than one percent change in RMS errors [3]. This is partially a function of using a simple scalar first order Gauss-Markov model to define the beam centroid dynamics [3,8]. Assuming the first order beam model proves to be adequate, this insensitivity was used to simplify the structure of the Meer filter by limiting the depth to  $D=1$ , and defining the filter gain,  $\mathbf{K}(r')$ , as a function of the residual,  $r'$  [3,8].

The mathematical development of the simplified algorithm can be established in the following manner [3]. If the elemental Snyder-Fishman filter assumes that the event was signal-induced, the beam state estimate is

$$\hat{\mathbf{x}}_1(t_i^+) = \hat{\mathbf{x}}_1(t_i^-) + \mathbf{K}(t_i)[\mathbf{r} - \mathbf{H}_1(t_i)\hat{\mathbf{x}}_1(t_i^-)] \quad (19)$$

The probability it was in fact a signal-induced event is

$$p_1(t_i) = \hat{\lambda}_S(t_i, r_i, \hat{\mathbf{x}}(t_i)) / \hat{\lambda}(t_i, r_i, \hat{\mathbf{x}}(t_i)) \quad (20)$$

using the notation of Eq. (15). If the elemental Snyder-Fishman filter assumed that the event was noise-induced, then  $\hat{\mathbf{x}}_2(t_i^+) = \hat{\mathbf{x}}_2(t_i^-)$ . The probability it was a noise-induced event is

$$p_2(t_i) = \hat{\lambda}_N(t_i, r_i) / \hat{\lambda}(t_i, r_i, \hat{\mathbf{x}}(t_i)) = 1 - p_1(t_i) \quad (21)$$

Therefore, the adaptive beam state estimate is

$$\begin{aligned} \hat{\mathbf{x}}_A(t_i^+) &= p_1(t_i)\hat{\mathbf{x}}_1(t_i^+) + p_2(t_i)\hat{\mathbf{x}}_2(t_i^+) \\ &= \hat{\mathbf{x}}_A(t_i^-) + p_1(t_i)\mathbf{K}(t_i)[\mathbf{r} - \mathbf{H}_1(t_i)\hat{\mathbf{x}}_1(t_i^-)] \end{aligned} \quad (22)$$

where  $\hat{\mathbf{x}}_A(t_i^-) = \hat{\mathbf{x}}_1(t_i^-) = \hat{\mathbf{x}}_2(t_i^-)$ . Thus, the algorithm involves a single Snyder-Fishman-like filter, but with a modified gain of  $[p_1(t_i)\mathbf{K}(t_i)]$ , and thus the gain is a function of the residual as seen in Fig. 3.

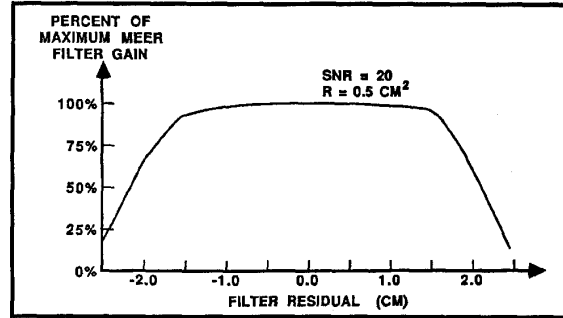


Figure 3. Meer Filter Gain

## CONTROLLER SYNTHESIS

If we can unrealistically assume perfect access to all the states, then we can develop an LQ optimal proportional-plus-integral controller [6]. This development, of course, assumes that both the beam and target models are represented by linear systems, and that a deterministic optimal control law can be derived so as to minimize the tracker error according to some quadratic cost function. The controller's gain is based on a backward Riccati difference equation, assuming all the particle beam and target states are perfectly known. Then, by "assumed" certainty equivalence [6], the "perfectly known" states are replaced by the state estimates provided by the Meer filter (beam states) and a Kalman filter (target states).

The target dynamics position process is modeled as the double integral of exponentially time-correlated acceleration; a third-order Markov process that is the output of a third order, linear, time-invariant shaping filter driven by stationary white Gaussian noise process,  $w_T(t)$ , that has a mean of zero and a variance of  $Q_T$  [3]. The state-space representation of this model is

$$\dot{\mathbf{x}}_T(t) = \mathbf{F}\mathbf{x}_T(t) + \mathbf{G}_T w_T(t) = \begin{bmatrix} 0 & 1 & 0 \\ 0 & 0 & 1 \\ 0 & 0 & -1/\tau_T \end{bmatrix} \mathbf{x}_T(t) + \begin{bmatrix} 0 \\ 0 \\ 1 \end{bmatrix} w_T(t) \quad (23)$$

where  $\mathbf{x}_T(t)$  is composed of the target position, velocity and acceleration states, and  $\tau_T$  is the target acceleration correlation time constant. The target position is measured as a sample-data function defined by

$$z(t_i) = \mathbf{H}_T(t_i)\mathbf{x}_T(t_i) + v(t_i) \quad (24)$$

where  $\mathbf{H}_T(t_i) = [1 \ 0 \ 0]$  and  $v(t_i)$  is a discrete-time zero-mean white Gaussian measurement corruption noise with a covariance  $R_T$ , and is assumed to be independent of the dynamics driving noise in Eq. (23). The discrete

Kalman filter propagation and update equations are used to provide the controller with target state estimates,  $\hat{\mathbf{x}}_T(t_i)$ .

For a sample data control system, we can choose an appropriate sample period (the controller sampling rate is independent of the beam measurement process), and generate an equivalent discrete time system model [6]. The linear discrete-time state equation that was used to model the beam is

$$\mathbf{x}_B(t_{i+1}) = \Phi_B(t_{i+1}, t_i) \mathbf{x}_B(t_i) + \mathbf{B}_d(t_i) u_B(t_i) + \mathbf{w}_{Bd}(t_i) \quad (25)$$

where  $\Phi_B(t_{i+1}, t_i)$  is the beam state transition matrix derived from  $F = -1/\tau_B$  (see Eq. (3)),  $\tau_B$  is the beam time constant,  $\mathbf{x}_B(t_i)$  is the beam's position,  $u_B(t_i)$  is the control applied over the next sample period, and  $\mathbf{w}_{Bd}(t_i)$  is a zero mean white Gaussian discrete-time stochastic process of strength  $Q_d$ , where:

$$Q_d = G^2 \int_{t_i}^{t_{i+1}} \Phi_B^2(t_{i+1}, \tau) d\tau$$

The linear discrete-time state equation that defines the target dynamics is

$$\mathbf{x}_T(t_{i+1}) = \Phi_T(t_{i+1}, t_i) \mathbf{x}_T(t_i) + \mathbf{G}_{Td} \mathbf{w}_{Td}(t_i) \quad (26)$$

where  $\Phi_T(t_{i+1}, t_i)$  is the state transition matrix associated with  $\mathbf{F}$  in Eq. (23).

The PI controller was selected on its ability to handle unmodeled step disturbances that arise from linearization. PI controller synthesis by LQ regulator techniques is accomplished by introducing an additional set of dynamic variables, with defining difference equations, which is then augmented to the original states. These additional variables can correspond to the pseudointegral of the regulation error,

$$q(t_i) = q(t_{i-1}) + [y_c(t_i) - y_r(t_i) - y_d] \quad (27)$$

where  $y_c(t_i) = \mathbf{C}_c(t_i) \mathbf{x}_B(t_i)$  is the controlled variable,  $y_r(t_i) = \mathbf{C}_r(t_i) \mathbf{x}_T(t_i)$  is the reference variable to be tracked, and  $y_d$  is any desired offset.

The PI control law is determined from the discretized, augmented system equation (see Eqs. (25) through (27))

$$\mathbf{x}_a(t_{i+1}) = \Phi_a \mathbf{x}_a(t_i) + \mathbf{B}_{da} u(t_i) + \mathbf{D}_a y_d + \mathbf{G}_{da} \mathbf{w}_{da}(t_i) \quad (28)$$

where  $\mathbf{x}_a(t_i) = [\mathbf{x}_B(t_i)^T \mathbf{x}_T(t_i)^T q(t_i)^T]^T$ , and is designed to minimize a quadratic cost in the tracking error defined as

$$e(t_i) = y_c(t_i) - y_r(t_i) \quad (29)$$

The PI tracker was restricted to a time-invariant system using constant weighting matrices. These restrictions along with a decision to ignore short

transients in Riccati solutions allow the problem to be solved using steady-state constant gains.

Thus, the "optimal" control law is

$$u(t_i) = -\mathbf{G}_c^* \mathbf{x}_a(t_i) + E y_d \quad (30)$$

where the controller's optimality is defined by minimizing the quadratic cost function,

$$J = E \left\{ \sum_{i=0}^N [\mathbf{x}_a^T(t_i) \mathbf{X}_a(t_i) \mathbf{x}_a(t_i) + U(t_i) u^2(t_i)] / 2 \right\} \quad (31)$$

which is designed to minimize the tracker error defined by Eq. (29).

Because the robustness analysis from the Monte Carlo simulation demonstrated that the controller was highly sensitive to the mismodeling of the target dynamics noise strength parameter,  $Q_T$ , this parameter was selected for on-line adaptive estimation. The importance of adaptively estimating this parameter is highlighted by the fact that the target, not the tracker, controls this parameter [3]. Parameter estimation was accomplished using a Multiple Model Adaptive Controller (MMAC) algorithm where the PI controller was replaced with a bank of PI controllers [1,2,5,6]. Each controller is based on a particular value of  $Q_{Tk}$ , where  $k$  identifies the controller within the bank. Within each controller, a state estimate,  $\hat{\mathbf{x}}_k(t_i^+)$ , is computed by a Kalman filter based on the parameter value,  $Q_{Tk}$ , and is multiplied by the appropriate steady-state gains based on the same parameter assumption (for this application, both  $\mathbf{G}_c$  and  $E$  are independent of the uncertain parameter). The result is an optimal control law conditioned on  $Q_{Tk}$  being the true parameter:

$$u_k(t_i) = -\mathbf{G}_c^* \hat{\mathbf{x}}_k(t_i^+) + E y_d \quad (32)$$

The adaptive control is generated by summing the probabilistically weighted values of  $u_k(t_i)$ ,

$$u(t_i) = \sum_{k=1}^K u_k(t_i) p_k(t_i) \quad (33)$$

The conditional probability,  $p_k(t_i)$ , is a recursive relationship derived using a Bayesian approach:

$$p_k(t_i) = \text{prob}\{\mathbf{a} = \mathbf{a}_k | \mathbf{Z}(t_i) = \mathbf{Z}_i\} \\ = \frac{f_{\mathbf{Z}(i)|\mathbf{a}, \mathbf{Z}(i-1)}(\zeta_i | \mathbf{a}_k, \mathbf{Z}_{i-1}) p_k(t_{i-1})}{\sum_{j=1}^K f_{\mathbf{Z}(i)|\mathbf{a}, \mathbf{Z}(i-1)}(\zeta_i | \mathbf{a}_j, \mathbf{Z}_{i-1}) p_j(t_{i-1})} \quad (34)$$

where  $\mathbf{Z}_i(t_i)$  is the measurement history, and  $\mathbf{a}$  is the uncertain parameter ( $\mathbf{a} = \mathbf{Q}_T$  for this model).

## DESIGN EVALUATION AND FINDINGS

The performance of the PI and MMAC tracker designs were evaluated using a Monte Carlo simulation of a one-dimensional detector array [3]. The Meier and Kalman filter performances were measured by the estimation error sample variance,  $P_e(t_i)$ , and the overall tracker performance was evaluated by the magnitude of the RMS tracker error,  $RMS_e(t_i)$ . The simulation was composed of 200 runs, each of 100 seconds in duration. The beam and target parameters were selected to portray a rather harsh target scenario as defined by the nominal conditions listed in Table 1. The cost weighting matrices were selected on their ability to minimize the RMS tracking error. A sensitivity analysis was performed to provide a baseline of the best possible controller performance provided the filters know the "real-world" environment. Then, a robustness analysis was performed to measure the ability of the controller to cope with a "real-world" environment that differs from the nominal parameter values assumed in the filter/controller design. In-depth sensitivity and robustness analyses were conducted on the  $\tau_B$ ,  $G$ ,  $R$ ,  $n$ ,  $SNR$ ,  $\tau_T$ ,  $Q_T$  and  $R_T$  parameters, and a summary of the results is presented in Table 1. Most of the parameters demonstrated good robustness characteristics. The two notable exceptions were the beam time constant ( $\tau_B$ ) and the target dynamics driving noise strength ( $Q_T$ ). All results were found using the simplified Meier filter ( $D=1$ ) as described by Eq. (22).

TABLE 1  
Summary of the Sensitivity and Robustness Analyses

Nominal Parameter Values	Scale Factor	Sensitivity $RMS_e$	Robustness $RMS_e$
1. $\tau_B = 20.0$ (sec)	10.0	+0.3%	-
	0.1	-0.7%	-
	1.05	-	very large
	1.02	-	+191.5%
	0.98	-	+195.2%
	0.96	-	very large
2. $G = 0.2$ (cm <sup>2</sup> /sec) <sup>1/2</sup>	10.0	+53.9%	+7.7%
	0.1	-1.2%	+0.3%
3. $\tau_T = 10$ (sec)	10.1	+9.7%	-1.3%
	0.1	-45.9%	+50.7%
4. $Q_T = 0.1$ (cm <sup>2</sup> /sec <sup>5</sup> )	10.0	+89.7%	+7.6%
	0.1	-40.3%	+39.4%
5. $R_T = 0.5$ (cm <sup>2</sup> )	10.0	+82.7	+41.4%
	0.1	-38.7	6.9%
6-8. $n = 1.0$ (events/sec) $R = 0.5$ (cm <sup>2</sup> ) $SNR = 20.0$		relatively insensitive to parameter variations	

Note: The controller and Kalman filter sample rates were 1.0 Hz.  
 $X_a: X_{11}=X_{22}=100, X_{12}=-100, X_{55}=10. U=1. B_d=0.97541.$

The beam time constant ( $\tau_B$ ) robustness results suggested a robustness stability problem and this is supported by the robustness analysis plots of  $RMS_e(t_i)$  (Fig. 4a), and the mean and standard deviation of the error between the true and filter beam states (Fig. 4b). The cause of this stability robustness problem is due to the combinational effect of the following three characteristics.

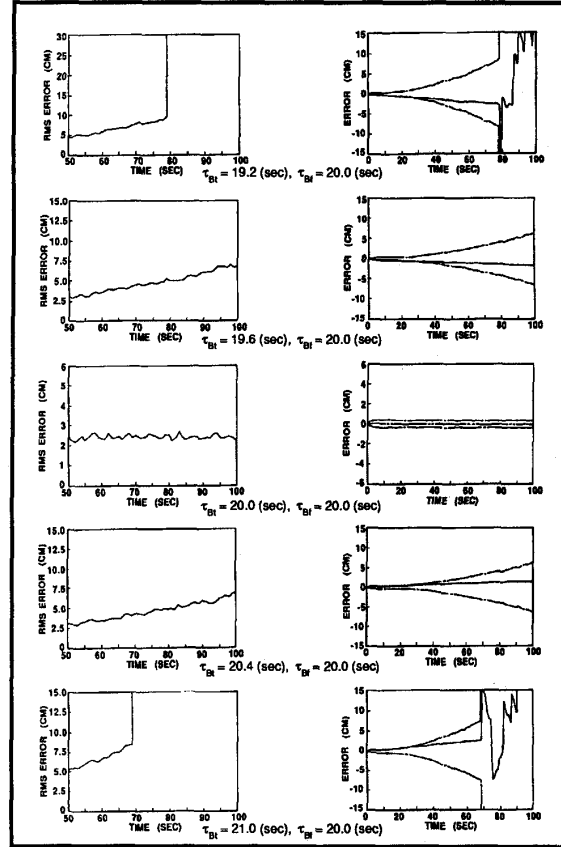


Figure 4. Beam Time Constant Robustness Results:  
(a) RMS Error and, (b) Mean and Standard Deviation of the Error between True and Filter Beam Position States.

First, the varying sample rate (based on the mean signal parameter rate of one signal event per second) could drive the controller unstable during the longer sample periods [3]. A rigorous proof of global stability for stochastic control system that uses either the simplified Meier filter or the Snyder-Fishman filter does not exist, and because the sample rate of the Meier filter is time-variant, the system does not yield to a classical stability analysis. Instead, an ad hoc method was employed wherein the effects of different sample rates were evaluated as though the sample rate was time-invariant, and zero-input stability analysis was used to evaluate the pole movement within the stochastic controller. The effects that a varying sample rate has on

the controller stability was evaluated by solving for the stochastic PI controller closed-loop transfer function for a range of different sample periods and Meer filter gains. As seen in Fig. 5, the results showed that, as the time between the last and next event grows, one of the poles of the controller migrates outside the unit circle. Two additional contributors to the instability of the controller are the magnitude of the Snyder-Fishman filter gain,  $K(t_i)$  in Eq. (10), and the magnitude of the beam propagation noise strength,  $G$  in Eq. (8). As either  $K(t)$  or  $G$  increases, the controller relies less on the Snyder-Fishman filter's internal dynamics model as a stabilizing factor under nominal conditions, and thus, the more likely the controller will become unstable during deterministically destabilizing sample periods [3]. Of course, such dependence on internal dynamics models is not overly desirable from a stability robustness point of view.

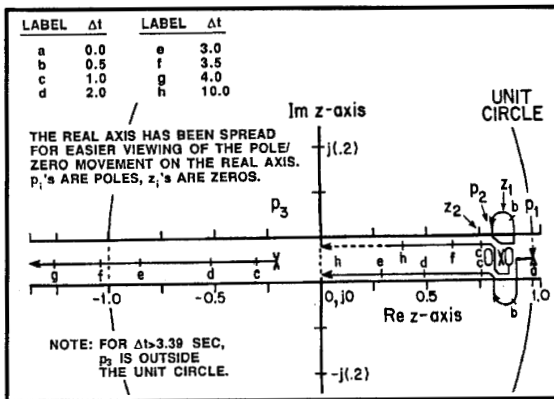


Figure 5. Zero-Input Stability Analysis of the Stochastic PI Controller: Varying the Meer Filter Sample Rate.

In addition to the varying sample period, the mismodeling of  $\tau_B$  can lead to large residuals, especially during the longer sample periods [3]. The magnitude of the residual could be controlled to some degree by on-line adaptive estimation of  $\tau_B$ . But this alone may not be sufficient. As the residuals increase, the Meer filter structure would assume that more of the incoming measurements were noise-induced, and the filter would inadvertently drive the Meer filter gain to zero (recall Fig. 3). Ideally, a large residual indicates that the event is most likely noise-induced, and the event receives a probabilistic weight as such. But, if the true center of the beam is offset from the filter's estimate of the center, then the Meer filter will begin to weight a large number of signal-induced events as being noise-induced (see Fig. 6). As more events are labeled noise-induced, the time between signal events will appear to increase, and the filter covariance will increase. Although this causes the elemental Snyder-Fishman filter to rely more on the incoming measurements, this is negated by the effect the probabilistic weight that the measurement was a signal-induced event,  $p_1(t_i)$  has on the Meer filter gain (recall Eq. (22)). As the filter beam center diverges from the true beam center,  $p_1(t_i)$  approaches zero and forces

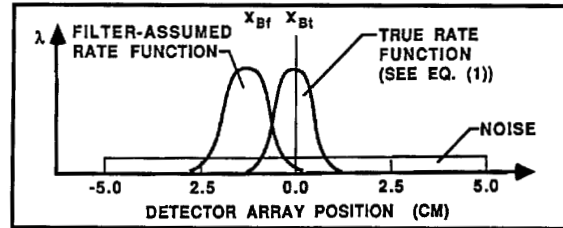


Figure 6. True Beam Offset from Filter Beam:  $R_t = R_f = 0.5$  cm,  $r^*(t_i) = 1.0$  cm

the Meer filter gain to zero, no new measurements are incorporated, and the filter never recovers.

This led to the hypothesis that some of the robustness can be recovered by computing the filter  $R$  (recall Eq. (11)) as a function of some weighted temporal average of the previous  $N$  squared residuals [3]. By increasing the filter  $R$  when the most recent residuals are consistently larger than originally anticipated, the Meer filter is told to look for the signal-induced events across a larger section of the detector (see Fig. 7). The advantage of this concept is that most of the signal-induced events can be correctly treated as being signal-induced, and the filter should have much better robustness with respect to the mismodeling of the beam time constant. The robustness analysis found that the controller is rather insensitive to increases of the filter  $R$ , and although the larger filter  $R$  will cause the filter to weight more noise-induced events as signal-induced events, this should have no significant effect on the RMS tracking error.

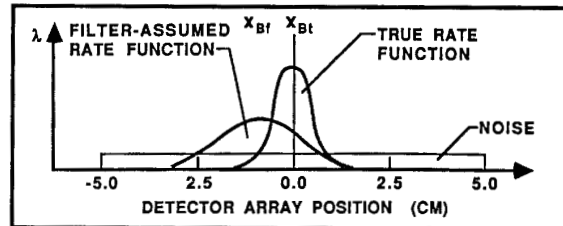


Fig. 7. True Beam Offset from Filter Beam:  $R_t = 0.5$  cm,  $R_f = 1.0$  cm,  $r^*(t_i) = 1.0$  cm

The implementation of a MMAC was viewed as a feasibility demonstration and only one parameter, the target dynamics driving noise strength ( $Q_T$ ), was selected for on-line adaptation. Each of the three elemental controllers was tuned to a specific value of  $Q_{TK}$ :  $Q_{T1} = 0.01$ ,  $Q_{T2} = 0.07$  and  $Q_{T3} = 1.0$ . The MMAC performed well against the unknowledgeable and non-adaptive controller based on a nominal parameter value, and closely approximated a fully knowledgeable filter (artificially informed of the "correct" parameter value) which was used as the baseline [3]. The results in Table 2 show that the adaptive controller does an excellent job of estimating the true  $Q_T$  representing the harsher maneuvering ( $Q_T = 1.0$ ), where performance

would be most critical. Large errors here could result in the loss of lock on the target. Also, the adaptive controller does a good job of adapting to the  $Q_T$  representing a more benign trajectory ( $Q_T=.01$ ). Much of the apparent drop in the MMAC's overall performance can be attributed to the occasional sluggishness of the adaptive mechanism when the controller is adapting to a decreasing  $Q_T$  (which could take anywhere from 6 to 69 controller sample periods). This is inherent in multiple model Bayesian estimation and has been noted in other studies of multiple model adaptive algorithms [4,7]. For comparison purposes, Table 2 also includes the results from the PI tracker.

TABLE 2: Results of the MMAC Analysis

	MMAC Results			PI Tracker Results		
	Baseline	Actual	Perfectly	Mismodeling of $Q_T$		
	Average RMS <sub>e</sub>	Average RMS <sub>e</sub>	Tuned $Q_T$ Average RMS <sub>e</sub>	$Q_T=0.01$	$Q_T=0.1$	$Q_T=1.0$
Overall Performance	3.139	3.546	-	-	-	-
Adapting to $Q_T=.01$	1.634	1.736	1.461	-	2.034	3.340
Adapting to $Q_T=1.0$	4.657	4.643	4.644	7.300	4.998	-

## CONCLUSION

The stochastic adaptive particle beam tracker is just one application of a class of stochastic controllers for which the feedback observations are modeled as a noise-corrupted space-time point process and where the time to the next event is unknown a priori. Both the non-adaptive PI controller and MMAC were synthesized based on assumed certainty equivalence, using LQ full-state feedback controller designs with simplified Meer filter feedback. The controller Monte Carlo analyses uncovered several important design issues. First, the varying sample rate can drive the controller unstable during the longer sample periods. Second, the mismodeling of the beam time constant  $\tau_B$  can lead to large residuals. Finally, as the residuals increase, the Meer filter structure will inadvertently drive the Meer filter gain towards zero. All three of these problems can be rectified by ensuring the design has a much higher mean signal rate parameter (to reduce the probability a controller will be driven unstable by a long sample period), by developing on-line adaptive estimation of  $\tau_B$  (to reduce the large residuals), and by on-line computing of the filter R as a time-weighted average of the recent filter squared residuals (to prohibit the Meer filter from erroneously driving the filter gain to zero).

## REFERENCES

- [1] M. Athans, and C. B. Chang, Adaptive Estimation and Parameter Identification Using Multiple Model Estimation Algorithm, ISD-TR-76-184, Tech. Note 1976-28. Lincoln Laboratory, Lexington, Massachusetts, June 1976.
- [2] J. G. Deshpande, T. N. Upadhyay, and D. G. Lainiotis, "Adaptive Control of Linear Stochastic Systems," *Automatica*, 9: 107-116 (January 1973).
- [3] B. A. Johnson, *Stochastic Adaptive Particle Beam Tracker Using Meer Filter Feedback*, MS Thesis, School of Engineering, Air Force Institute of Technology (AU), Wright-Patterson AFB, Ohio, December 1986.
- [4] J. Korn, and L. Beean, "Application of Multiple Model Adaptive Estimation Algorithms to Maneuver Detection and Estimation," Technical Report TR-152, Alphatech, Inc., Burlington, Mass., June 1983.
- [5] P. S. Maybeck, *Stochastic Models, Estimation, and Control, Volume 2*. New York: Academic Press, 1982.
- [6] P. S. Maybeck, *Stochastic Models, Estimation, and Control, Volume 3*. New York: Academic Press, 1982.
- [7] P. S. Maybeck, and K. P. Hentz, "Investigation of Moving-Target Multiple Model Adaptive Algorithms," *Proceedings of the IEEE 24th Conference on Decision and Control*, pp. 1874-1881, IEEE Press, Fort Lauderdale, FL, Dec 85.
- [8] P. S. Maybeck, and W. L. Zicker, "MAE - Based Control with Space Time Point Process Observations," *IEEE Transaction on Aerospace and Electronic Systems*, AES-21: pp. 292-300 (May 1985).
- [9] D. E. Meer, *Multiple Model Adaptive Estimation for Space-Time Point Process Observations*, PhD Dissertation, School of Engineering, Air Force Institute of Technology (AU), Wright-Patterson AFB, Ohio, September, 1982.
- [10] S. R. Robinson, P. S. Maybeck, and J. M. Santiago Jr., "Tracking a Swarm of Fireflies in the Presence of Stationary Stragglers", *Proceedings of the 1979 International Symposium on Information Theory*, Grignano, Italy, June 1979.
- [11] G. Rohringer, *Particle Beam Diagnostics by Resonant Scattering*, 1 June 1977-30 November 1977. Contract DASG60-77-C-0120. General Research Corporation, Santa Barbara, CA, December 1977.
- [12] D. C. Snyder, and P. M. Fishman, "How to Track a Swarm of Fireflies by Observing Their Flashes," *IEEE Transactions on Information Theory*, IT-21: 692-695 (Nov 1975).